

Electronic Supporting Information (ESI) for Inorganic Chemistry Frontiers

## Hexagonal Co<sub>6</sub> and Zigzag Co<sub>4</sub> Clusters

### Based Magnetic MOFs with *pcu* Net for Selective Catalysis

Ru-Xin Yao, Xiao-Hui Qiao, Xin Cui, Xiao-Xia Jia and Xian-Ming Zhang\*

*Department of Chemistry & Material Science,*

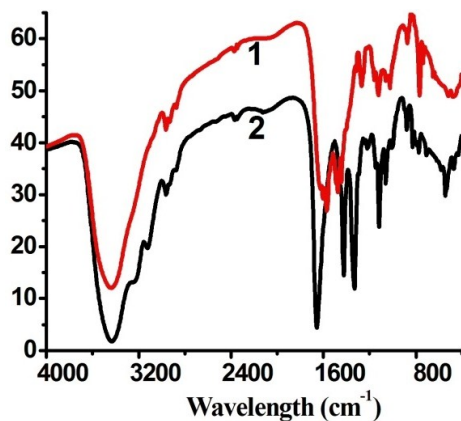
*Shanxi Normal University, Linfen 041004, P. R. China*

#### Supplementary Index

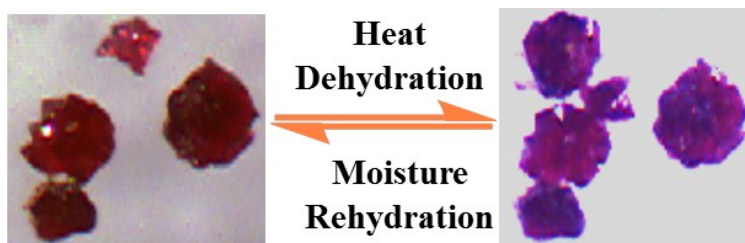
1. **Fig. S1** IR spectra of **1** and **2**.
2. **Fig. S2** Crystal photographs of **1** and activated **1** at heat and moisture conditions, respectively.
3. **Fig. S3** Four coordination modes of Hpimdc<sup>2-</sup> ligands.
4. **Fig. S4** Contact angle images of water (a)/ethanol (b) droplets balanced on the powders of **1**.
5. **Fig. S5** (a) Co<sub>6</sub>(pimdc)<sub>6</sub> unit linked with six Co<sub>6</sub> unit through Co<sub>2</sub> atoms in **1**, (b) 2D rhombic grid along *c*-axis direction in **2** (propyl group is deleted for clarity).
6. **Fig. S6** The TG/DTA plots of **1** and **2**.
7. **Fig. S7** The PXRD patterns of simulated and experimental for **1** and **2**, and that of after five catalytic cycles for catalyst **1**.
8. **Fig. S8** Temperature dependence of the susceptibility in different applied magnetic fields for **2**
9. **Fig. S9** N<sub>2</sub> sorption isotherms for **1** at 77 K
10. **Fig. S10** The allylic oxidation of cyclohexene with activated **1** as catalyst (black) and filtration of **1** (gray).
11. **Table S1**. The optimization of reaction condition for the allylic oxidation of cyclohexene with activated **1** as catalyst.
12. **Table S2**. Comparison catalytic performances of activated **1** with other catalysts

in the allylic oxidation of cyclohexene

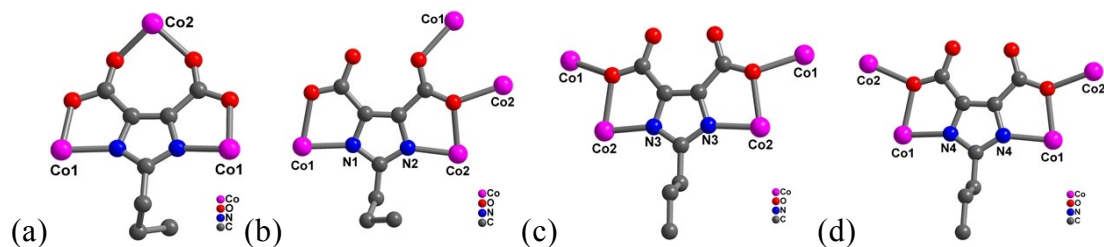
13. **Table S3.** Bond lengths [ $\text{\AA}$ ] and angles [deg] data for **1** and **2**



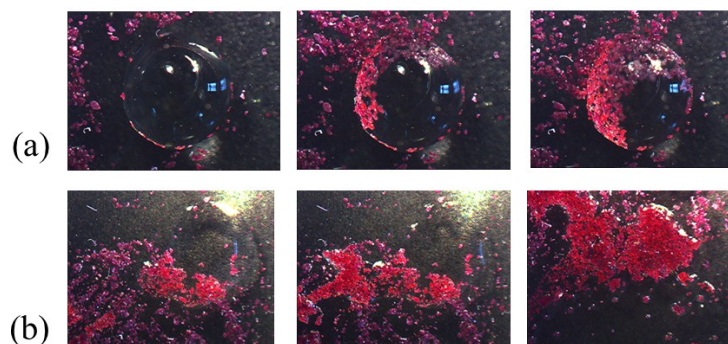
**Fig. S1** IR spectra of **1** and **2**.



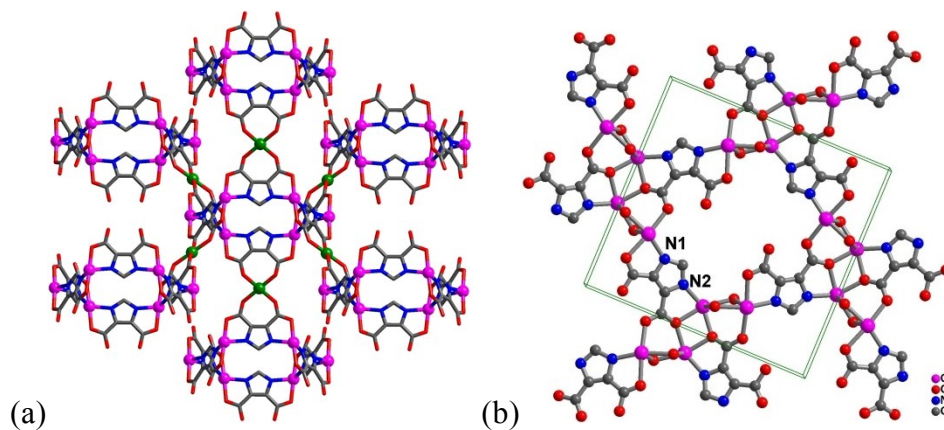
**Fig. S2** Crystal photographs of **1** and activated **1** at heat and moisture conditions, respectively.



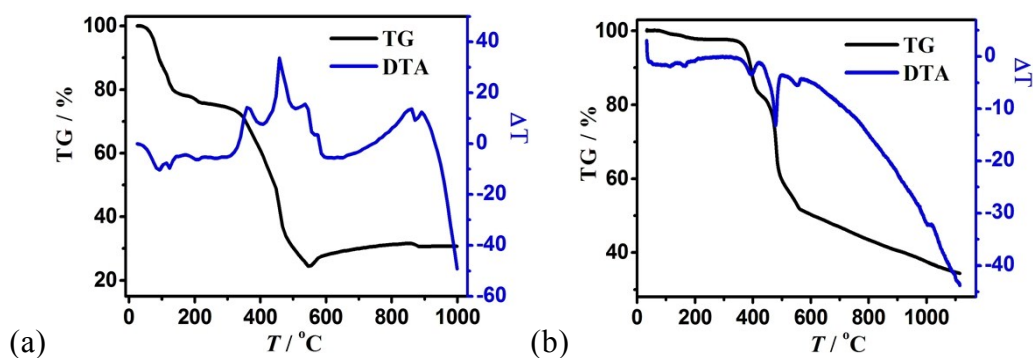
**Fig. S3** Four coordination modes of Hpimdc<sup>2-</sup> ligands, (a)  $\mu_3$ - $kN,O: kO',O''$ :  $kN',O'''$ , (b)  $\mu_4$ - $kN,O: kO': kO'': kN',O''$ , (c,d)  $\mu_4$ - $kN,O: kO: kO': kN',O'$ .



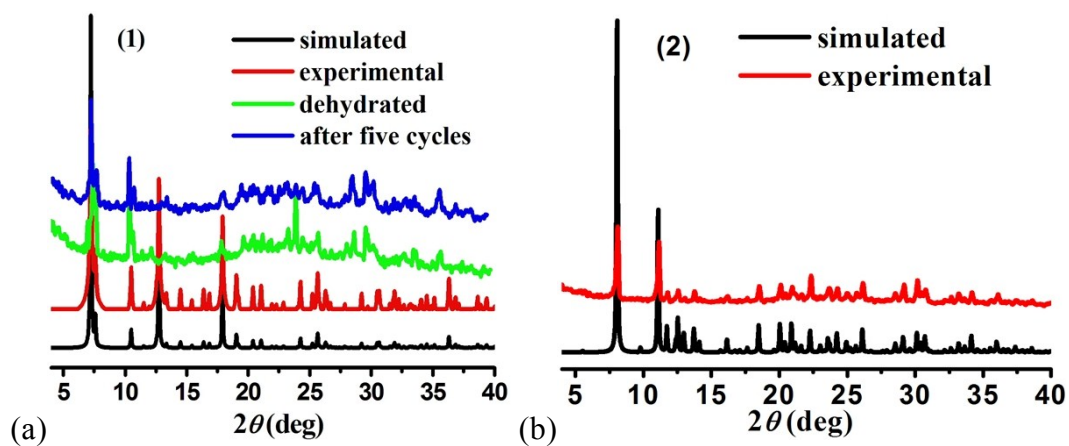
**Fig. S4** Contact angle images of (a) water and (b) ethanol droplets balanced on the powders of **1**.



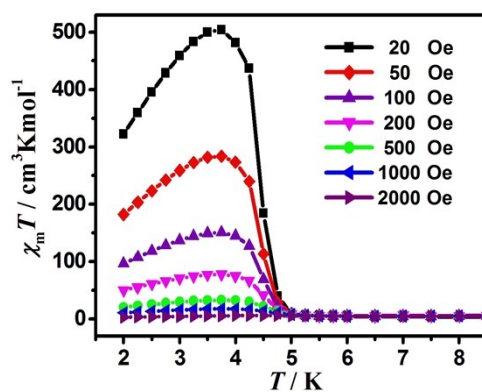
**Fig. 5** (a)  $\text{Co}_6(\text{pimdc})_6$  unit linked with six  $\text{Co}_6$  unit through  $\text{Co}_2$  atoms in **1**, (b) 2D rhombic grid along  $c$ -axis direction in **2** (propyl group is deleted for clarity).



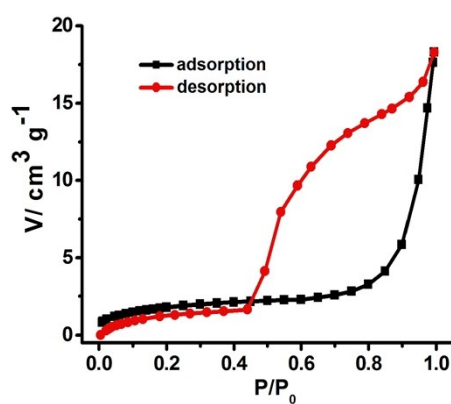
**Fig. S6** The TG/DTA plots of **1** and **2**.



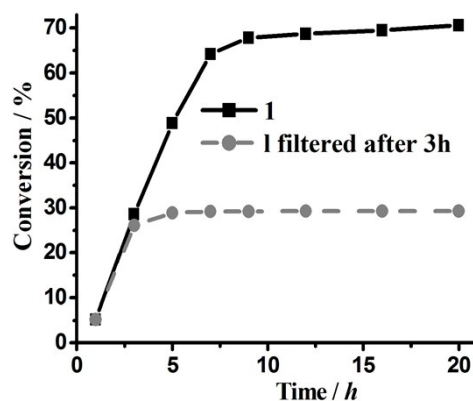
**Fig. S7** The PXRD patterns of simulated and experimental for **1** and **2**, and that of after five catalytic cycles for catalyst **1**.



**Fig. S8** Temperature dependence of the susceptibility in different applied magnetic fields for **2**.

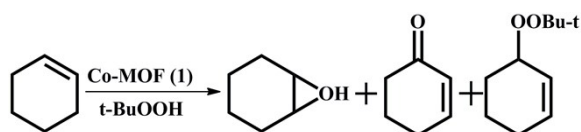


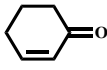
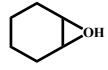
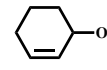
**Fig. S9** N<sub>2</sub> sorption isotherms for **1** at 77 K.



**Fig. S10** The allylic oxidation of cyclohexene with activated **1** as catalyst (black) and filtration of **1** (gray).

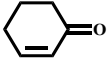
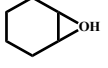
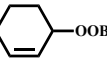
**Table S1.** The optimization of reaction condition for the allylic oxidation of cyclohexene with activated **1** as catalyst.



Entry	Particle	Temp. (°C)	Cat (mmol)	Con (%)	Selectivity (%)			TON <sup>b</sup>
								
					A	B	C	
1	unground <sup>a</sup>	50	0.15	28.6	48.3	28.6	23.1	91
2	ground	50	0.15	37.5	51.8	26.4	21.8	103
3	ground	50	0.10	41.6	54.6	29.7	15.7	118
4	ground	50	0.05	31.8	46.3	28.1	20.6	96
5	ground	60	0.10	56.4	57.8	25.3	17.9	123
6	ground	70	0.10	70.6	61.2	23.5	15.3	148
7	ground	80	0.10	25.6	46.9	27.4	22.9	85
8	ground	70	0.10 (hydrated <b>1</b> )	3.8	4.2	2.8	1.2	34
9	ground	70	0.10 ( <b>2</b> )	3.3	3.7	2.3	1.1	30
10	-----	70	-----	1.8	3.2	2.1	0.9	28

<sup>a</sup>Reaction conditions: cyclohexene (3.6 mmol), *t*-BuOOH (12 mmol), 1,2,4-trichlor-obenzene (1 mmol; as internal standard), Temp = 70°C, solvent-free. <sup>b</sup>TON (turnover number) = moles converted / moles of active Co sites. Entry 6 is the optimization of reaction condition.

**Table S2.** Comparison catalytic performances of activated **1** with other catalysts in the allylic oxidation of cyclohexene

Catalyst	<i>T</i> , °C (time, h)	Solvent	Con (%)	Selectivity (%)			Ref
							
				A	B	C	
activated <b>1</b>	70 (20)	free	70.6	61.2	23.5	15.3	
TM salts (Co)	homogeneous		> 99	50			[24]
Fe <sup>III</sup> /SiO <sub>2</sub>	78 (10)	CH <sub>3</sub> CN	98	76	5	--	[25]
Co-MOF	35 (24)	CH <sub>3</sub> CN	35	16	--	76	[26]
Cr-MIL-101	60 (16)	free	16	56	--	6	[27]

**Table S3.** Bond lengths [ $\text{\AA}$ ] and angles [deg] for **1** and **2**.

<b>Compound 1</b>			
Co(1)-N(1)	2.0673(19)	Co(2)-O(2b)	2.0361(16)
Co(1)-N(2a)	2.0638(18)	Co(2)-O(2)	2.0361(16)
Co(1)-O(4a)	2.1332(16)	Co(2)-O(3b)	2.0785(16)
Co(1)-O(1)	2.1451(16)	Co(2)-O(3)	2.0784(16)
Co(1)-O(1w)	2.1650(17)	Co(2)-O(3wb)	2.148(2)
Co(1)-O(2w)	2.1861(17)	Co(2)-O(3w)	2.148(2)
N(2a)-Co(1)-N(1)	104.98(8)	O(2b)-Co(2)-O(2)	180.00(0)
N(2a)-Co(1)-O(4a)	78.37(6)	O(2b)-Co(2)-O(3b)	93.36(7)
N(1)-Co(1)-O(4a)	106.86(7)	O(2)-Co(2)-O(3b)	86.65(7)
N(2a)-Co(1)-O(1)	100.97(7)	O(2b)-Co(2)-O(3)	86.64(7)
N(1)-Co(1)-O(1)	78.48(6)	O(2)-Co(2)-O(3)	93.36(7)
O(4a)-Co(1)-O(1)	174.64(6)	O(3b)-Co(2)-O(3)	180.00(0)
N(2a)-Co(1)-O(1W)	91.97(7)	O(2b)-Co(2)-O(3Wb)	87.99(7)
N(1)-Co(1)-O(1W)	159.82(7)	O(2)-Co(2)-O(3Wb)	92.00(7)
O(4a)-Co(1)-O(1W)	86.97(7)	O(3)-Co(2)-O(3Wb)	91.85(8)
O(1)-Co(1)-O(1W)	87.74(6)	O(3b)-Co(2)-O(3Wb)	88.15(8)
N(2a)-Co(1)-O(2W)	167.02(7)	O(2b)-Co(2)-O(3W)	92.01(7)
N(1)-Co(1)-O(2W)	83.57(7)	O(2)-Co(2)-O(3W)	88.00(7)
O(4a)-Co(1)-O(2W)	89.89(6)	O(3b)-Co(2)-O(3W)	91.85(8)
O(1)-Co(1)-O(2W)	90.20(6)	O(3)-Co(2)-O(3W)	88.15(8)
O(1W)-Co(1)-O(2W)	81.80(7)	O(3Wb)-Co(2)-O(3W)	180.00(0)

Symmetry codes: a)  $x-y+2/3$ ,  $x+1/3$ ,  $4/3-z$ ; b)  $1-x$ ,  $1-y$ ,  $1-z$ .

<b>Compound 2</b>			
Co(1)-N(1)	2.058(4)	Co(2)-N(2b)	2.052(4)
Co(1)-N(4)	2.092(4)	Co(2)-N(3)	2.074(3)
Co(1)-O(5)	2.146(3)	Co(2)-O(8)	2.102(3)
Co(1)-O(8)	2.171(3)	Co(2)-O(1a)	2.135(3)
Co(1)-O(2a)	2.178(3)	Co(2)-O(1b)	2.141(3)

Co(1)-O(4)	2.225(4)	Co(2)-O(5)	2.174(3)
N(1)-Co(1)-N(4)	107.03(16)	N(2b)-Co(2)-N(3)	101.43(14)
N(1)-Co(1)-O(5)	97.14(14)	N(2b)-Co(2)-O(8)	90.13(14)
N(4)-Co(1)-O(5)	152.84(14)	N(3)-Co(2)-O(8)	155.60(13)
N(1)-Co(1)-O(8)	165.75(16)	N(2b)-Co(2)-O(1a)	149.15(14)
N(4)-Co(1)-O(8)	77.88(13)	N(3)-Co(2)-O(1a)	98.73(13)
O(5)-Co(1)-O(8)	75.79(12)	O(8)-Co(2)-O(1a)	80.66(12)
N(1)-Co(1)-O(2a)	105.41(15)	N(2b) -Co(2)-O(1b)	78.16(13)
N(4)-Co(1)-O(2a)	95.76(15)	N(3)-Co(2)-O(1b)	98.67(12)
O(5)-Co(1)-O(2a)	89.45(12)	O(8)-Co(2)-O(1b)	104.75(12)
O(8)-Co(1)-O(2a)	87.09(13)	O(1a) -Co(2)-O(1b)	75.91(14)
N(1)-Co(1)-O(4)	78.39(15)	N(2b) -Co(2)-O(5)	119.48(14)
N(4)-Co(1)-O(4)	88.44(16)	N(3)-Co(2)-O(5)	78.97(12)
O(5)-Co(1)-O(4)	84.38(14)	O(8)-Co(2)-O(5)	76.63(12)
O(8)-Co(1)-O(4)	88.50(13)	O(1a) -Co(2)-O(5)	87.10(12)
O(2a)-Co(1)-O(4)	173.15(14)	O(1b)-Co(2)-O(5)	162.35(12)

Symmetry codes: a)  $-x+1/2, y+1/2, z$ ; b)  $x-1/2, -y+1/2, z$ .